Journal of Alloys and Compounds 509S (2011) S464–S467

Contents lists available at ScienceDirect

Journal of Alloys and Compounds

journal homepage: www.elsevier.com/locate/jallcom

2Mg–Fe and 2Mg–Fe + 5%C mixtures processed by hot extrusion: Influence of carbon on hydrogen sorption properties

R. Cerutti[a], G.F. de Lima[b], Cláudio S. Kiminami[a], W.J. Botta[a], A.M. Jorge Junior[a,*]

[a] Department of Materials Engineering, Federal University of São Carlos, Via Washington Luiz, km 235, 13565-905 São Carlos, SP, Brazil
[b] PPGCEM, Federal University of São Carlos, São Carlos, SP, Brazil

ARTICLE INFO

Article history:
Received 1 July 2010
Received in revised form 9 October 2010
Accepted 8 November 2010
Available online 13 November 2010

Keywords:
2Mg–Fe alloy
Hot extrusion
Hydrogen storage

ABSTRACT

Mg is a promising candidate material for hydrogen storage but its application is restricted by high sorption temperatures and slow sorption kinetics. Major efforts have focused on overcoming these two obstacles. Alloying, nanostructuring and/or catalysts, particularly at low temperatures, have considerably improved the hydrogenation kinetics of Mg powders. Further investigation is still desirable to reach the same properties for bulk materials because hydrogen desorption in bulk Mg-based systems still remains at a critical high temperature, and this, represents a major obstacle to their practical application. The aim of this work was to evaluate the reduction in desorption temperature and the increase in hydrogenation kinetics of bulk Mg-based composites in response to the following variables: particle/grain size, density of defects, the use of iron as catalyst, volume modifications, and the presence of carbon as a pore-confining element. We compared the behavior of 2Mg–Fe powder mixtures produced by high-energy ball milling processed as follows to produce bulk samples: (i) hot extrusion of 2Mg–Fe with extrusion ratio of 5/1 (S-1), (ii) hot compaction of 2Mg–Fe (S-2), and (iii) hot compaction of ball-milled 2Mg–Fe + 5%C, all processed at 300 °C (S-3). The samples were activated and subsequently hydrogenated at 15 bar, sample S-1 for 24 h and sample S-2 and S-3 for 5 h. After the hydrogenation treatments, the complex hydride Mg_2FeH_6 was formed in all the conditions. Desorption temperatures varied according to the processing conditions and the results indicated that porosity was an important factor, as it was the addition of carbon, which accelerated the desorption kinetics.

1. Introduction

Hydrogen storage materials for mobile applications, e.g., in hydrogen-fueled vehicles, should present high gravimetric and volumetric hydrogen capacities. Metal hydrides (solid state storage) are safer due to their stability at room temperature, and more efficient than gas or liquid state storage. Magnesium and Mg-based alloys are promising materials for hydrogen storage in the solid state due to their efficiency in mass and volume of storage, their safety, since the decomposition of hydrides is usually an endothermic process, and also their easier handling at ambient temperature than other storage methods. Magnesium hydride (MgH_2) has the highest gravimetric storage capacity (~7.6 wt% of H), and among the Mg-based hydrides, ternary intermetallic Mg_2FeH_6 has a high capacity of 5.5 wt% of H and the highest volumetric storage capacity of 150 kg/l of H, which is almost double that of liquid hydrogen. However, for possible practical applications, the hydrogen sorption rates of Mg/Mg-based alloy need to be faster, the temperatures for these reactions should decrease, and also the reactivity toward air and oxygen should be lower [1]. With the development of nanostructured materials processed by high-energy ball milling (HEBM) in the 1990s, reasonable sorption kinetics was observed in Mg-based hydrides [2]. The addition of catalyst elements and the formation of nanocomposite materials also contributed to enhance their kinetics [3,4].

The addition of Fe to MgH_2 was also found to improve the hydrogen absorption properties, but not the hydrogen desorption kinetics [5]. Further studies focused on the synthesis of the complex Mg_2FeH_6 hydride [6,7]. More recently, the various techniques of severe plastic deformation (SPD) have been also used in the development of Mg-based hydrides [8,9]. These SPD techniques applied to Mg-based systems have resulted in improved hydrogen sorption properties and kinetics.

The aim of this work was to evaluate the reduction in desorption temperature and the increase in the hydrogenation kinetics of bulk Mg-based composites in response to the following variables: particle/grain size, density of defects, the use of iron as catalyst, volume modifications, and the presence of carbon as a pore-confining element. We compared the behavior of 2Mg–Fe powder mixtures produced by high-energy ball milling processed as follows to pro-

---

* Corresponding author. Tel.: +55 16 33518531; fax: +55 16 33615404.
E-mail address: moreira@dema.ufscar.br (A.M. Jorge Junior).

0925-8388/$ – see front matter © 2010 Elsevier B.V. All rights reserved.
doi:10.1016/j.jallcom.2010.11.035

duce bulk samples: (i) hot extrusion of 2Mg–Fe, (ii) hot compaction of 2Mg–Fe, and (iii) hot compaction of ball milled 2Mg–Fe + 5%C. The hydrogenation properties of the samples extruded under different conditions were also investigated.

2. Experimental

Pure magnesium (+20–100 mesh, 99.98%, Alfa Aesar) and Fe (−20 mesh, 99.998%, Alfa Aesar) were mixed into the 2Mg–Fe (at.%) composition for 12 h by means of high-energy ball milling using the SPEX 8000M Mixer/Mill, in the following conditions: 0.395 g of material, 1080 shake cycles/min, ball-to-powder ratio of 40:1 (8 chromium steel balls), under argon gas atmosphere. Samples of 2Mg–Fe + 5%C (Carbon: <200 mesh, 99.9995%, Alfa Aesar) were prepared similarly, but with the addition of 5%C to the former powder, followed by milling for 30 min.

Cold-pressed preforms were produced using powders with particle sizes of up to 120 μm. The preforms were then processed in the following conditions: (i) 2Mg–Fe was hot-extruded at 300 °C at a ram speed of 1 mm/min and an extrusion ratio of 5/1 (S-1), (ii) 2Mg–Fe (S-2) and 2Mg–Fe + 5%C (S-3) were hot compacted at 300 °C in same matrix as that of condition (i). In these two last conditions, the samples were pressed continually up to a load increase of 10%. The bulk samples produced in all the conditions were reactivated (30 bar of H_2, 1 h, 300 °C) and subsequently hydrogenated at 15 bar, sample S-1 for 24 h and samples S-2 and S-3 for 5 h, all at 300 °C.

The microstructure was characterized by transmission electron microscopy (TEM), FEI-TECNAI G2-F20, equipped with an Energy-Dispersive X-ray Spectrometer (EDS), EDAX-EDAMIV/DPP2, STEM module (scanning transmission electron

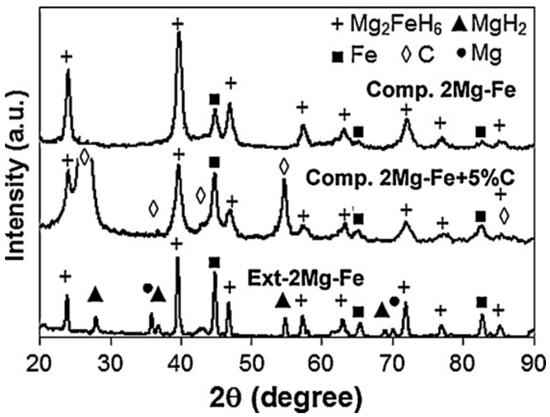

Fig. 1. XRD patterns of the samples extruded and treated by hydrogen absorption in the following conditions: (S-1) 2Mg–Fe hot-extruded and hydrogenated under 15 bar of H_2 for 24 h. (S-3) 2Mg–Fe + 5%C hot-compacted and hydrogenated under 15 bar of H_2 for 5 h. (S-2) 2Mg–Fe hot-compacted and hydrogenated under 15 bar of H_2 for 5 h.

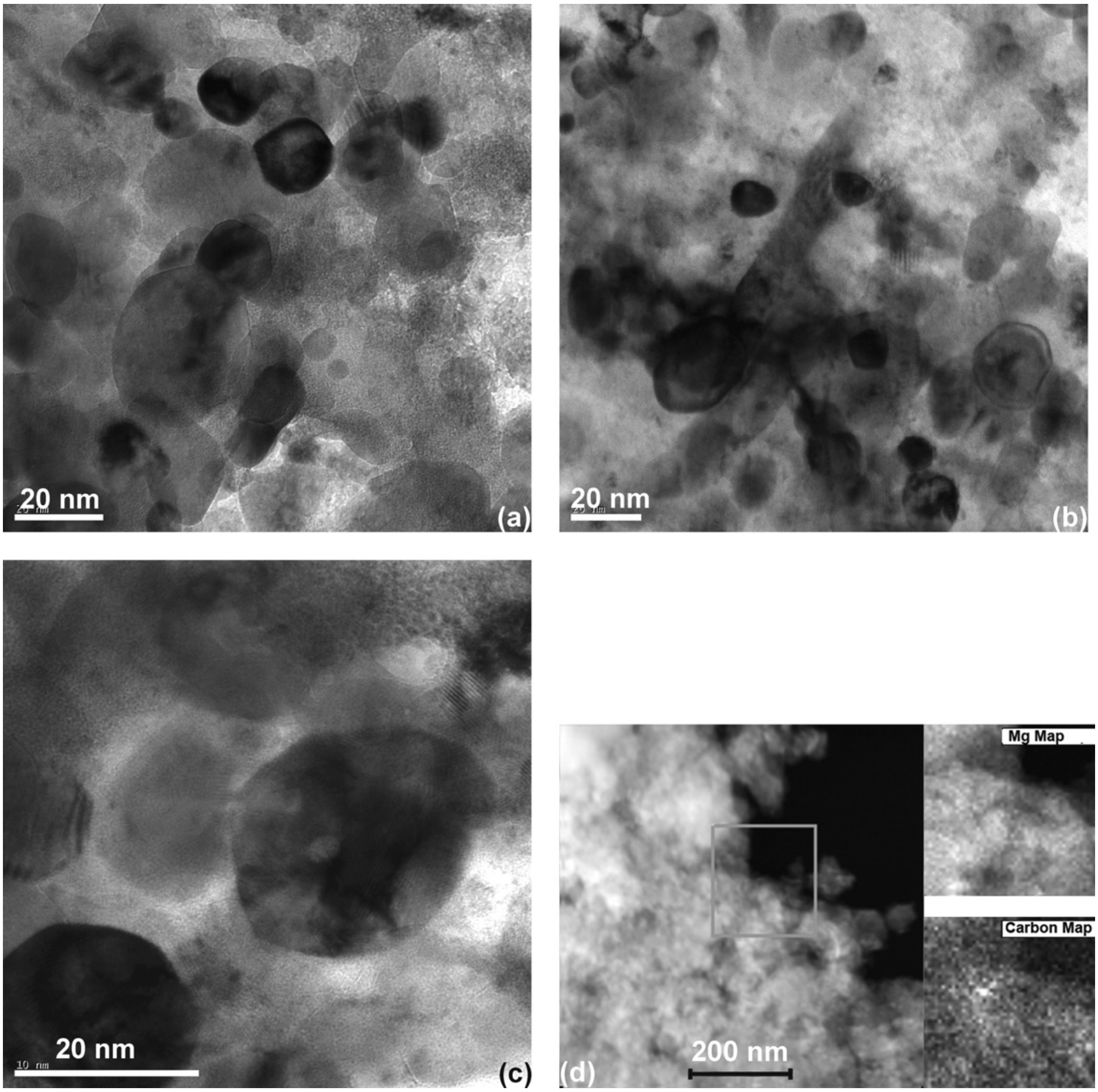

Fig. 2. (a), (b) and (c) TEM Bright Field images of samples S-1, S-2 and S-3, respectively. (d) STEM HAADF (left) and X-ray mapping of Mg and carbon images (right) of sample S-3.

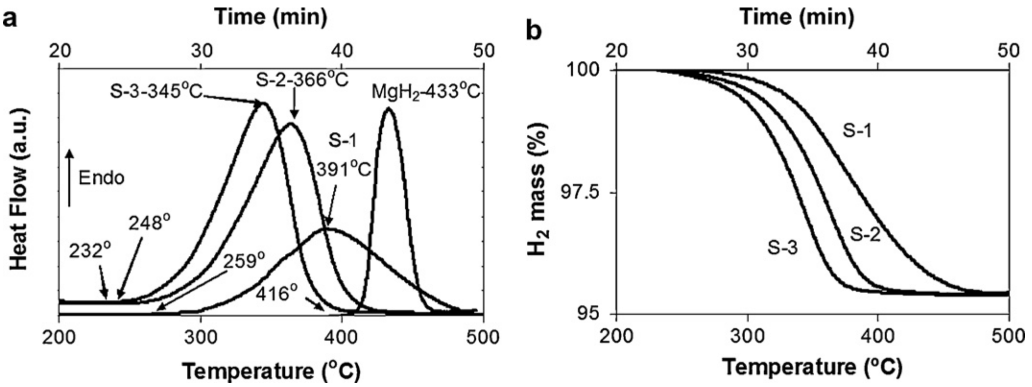

Fig. 3. STA measurements: (a) differential scanning calorimetry for samples S-3, S-2, S-1 and commercial MgH_2, respectively. (b) Thermogravimetry for samples S-3, S-2, S-1, respectively.

microscopy), and HAADF (high angle annular dark filed – Z-contrast). For preparing TEM specimens from the bulk samples, the extruded were cut and ground in a 190 ml unglazed porcelain mortar and wooden pestle in an *isopropyl alcohol* medium and, subsequently, droplet in a 3 mm–200 mesh carbon copper grid.

The phases were identified by X-ray diffraction (XRD) using monochromatic Cu Kα radiation with an angular pass of 0.032° in a Rigaku DMAX diffractometer equipped with a C-monochromator. Crystallite size was estimated by the Hall–Williamson methodology [10].

The thermal and thermogravimetric properties of the compacts were analyzed using a Netzsch DSC-TGA 404 calorimeter. Hydrogen desorption temperatures were measured during continuous heating of 12 mg of hydrides at a constant heating rate of 10 °C/min, using purified and dried argon gas in an overflow regime.

3. Results and discussion

Cold-pressing to produce the preforms resulted in relative densities of around 0.51. The relative density of the samples increased as follows: 0.85 for sample S-1, and 0.65 for samples S-2 and S-3. The XRD patterns of the powders and the 2Mg–Fe mixtures processed by hot-extrusion and hot-compaction revealed the presence of hcp-Mg and bcc-Fe. The XRD patterns of the powders and the 2Mg–Fe + 5%C mixtures processed by hot-extrusion and hot-compaction revealed the presence of hcp-Mg, bcc-Fe and carbon.

Fig. 1 shows the XRD patterns of processed samples after the heat treatment to absorb hydrogen. The phases were indexed. The analysis of S-1, the 2Mg–Fe mixture extruded and hydrogenated under 15 bar of H_2 for 24 h, indicated Fe, MgH_2 and Mg_2FeH_6. Sample S-2, the 2Mg–Fe mixture compacted and hydrogenated under 15 bar of H_2 for 5 h, showed only Fe and Mg_2FeH_6. The analysis of sample S-3, 2Mg–Fe + 5%C compacted and hydrogenated as in S-2, indicated only carbon, Mg_2FeH_6 and a residual portion of Fe. The estimated grain size in all the samples was about 20 nm for Fe and 30 nm for Mg.

Fig. 2 shows images of the hydrogenated samples. Fig. 2(a)–(c) shows TEM Bright Field images of samples S-1, S-2 and S-3, respectively. Fig. 2(d) shows STEM HAADF (left) and X-ray mapping of Mg and carbon images (right) of sample S-3. The main features that can be observed in Fig. 2 are: (i) the grain size is consistent with the crystallite size determined by the Hall–Williamson methodology; (ii) the iron (black regions in Fig. 2(a)–(c) and white regions in Fig. 2(d)) is well distributed in all the samples; (iii) Fig. 2(c) indicates that carbon is well distributed over the particle surfaces.

Fig. 3 shows STA results of the hydrogenated samples. Fig. 3(a) depicts the desorption temperatures of extruded and compacted samples compared with commercial MgH_2 powder. The data indicate a nucleation time prior to the onset of dehydrogenation. The onset and peak temperatures of S-1, S-2 and S-3 occurred at about 259–391 °C, 248–366 °C and 232–345 °C, respectively. All the samples presented lower onset temperatures than the commercial MgH_2 powder, i.e., about 157 °C, 168 °C and 184 °C lower for S-1, S-2 and S-3, respectively. The onset behavior can be explained by the nanostructuring, which increased porosity in the same sequence, and by the presence of carbon in S-3. Fig. 3(a) also shows that the desorption kinetics of these samples are still slow when compared to the MgH_2 powders, but that they increase in the sequence of S-1 to S-3. There are at least two possible explanations for the significant effect of carbon additive on the hydrogen storage of Mg: (i) the carbon likely segregates at the grain boundaries (Fig. 2(d)) during ball milling, thereby increasing hydrogen diffusion at the boundaries; (ii) sublayer carbon atoms may be formed by incorporation into Mg and Fe structures during ball milling, enhancing the atomic hydrogen diffusion from surface to bulk Mg + Fe.

The results depicted in Fig. 3(a) and (b) indicate that the addition of Fe is expected to significantly reduce the dissociation barriers for H_2 dissociation as well as the onset temperature of dehydrogenation (S-1 and S-2). This may indicate that the dissociation of H_2 and recombination of H to H_2 occur mainly in association with iron, due to its lower barrier than that of pure magnesium, even with the small percentage of Fe present. Possibly, this suggests that Fe catalyzes mainly the dissociation/recombination reaction barrier for H_2 while exerting a minor effect on other processes. Moreover, Fig. 3(b) also shows the faster dehydrogenation kinetics of sample S-3, which is visible along with the sigmoidal curves. Here, even with the presence of MgH_2 in S-1, which can accelerate the H_2 reactions, the combined effect of porosity and iron in sample S-2 and the combined effect of porosity, iron and carbon in sample S-3 seems to play a catalytic and diffusive role, considerably hastening the Mg–H reactions in what appears to be a more efficient way than when only iron and nanostructuring is employed for this same purpose. In addition, the thermogravimetric analyses (TG) (Fig. 3(b)) indicated that all the samples studied in this work presented a very good and equal percentage of hydrogen absorption, i.e., about 4.56%. However, it is very important to keep in mind that, unlike sample S-1, which was hydrogenated for 24 h, samples S-2 and S-3 were hydrogenated for only 5 h, again demonstrating the beneficial effect of porosity and the combination of porosity and carbon in these samples, respectively.

4. Conclusions

Desorption temperatures varied with the processing conditions and the results indicated that porosity was an important factor, which, allied to the addition of carbon, accelerated the desorption kinetics. This effect was also exhibited by the absorption kinetics of samples S-2 (hot-compacted 2Mg–Fe) and S-3 (hot-compacted 2Mg–Fe + 5%C), even with only 5 h of hydrogenation, compared to 24 h for sample S-1 (hot-extruded 2Mg–Fe).

Acknowledgements

The authors gratefully acknowledge the financial support of the Brazilian agencies FAPESP, CAPES, CNPq and FINEP.

References

[1] B. Sakintuna, F. Lamari-Darkrimb, M. Hirscher, International Journal of Hydrogen Energy 32 (2007) 1121–1140.
[2] S. Rivoirard, P. Rango, D. Fruchart, J. Charbonnier, D. Vempaire, Journal of Alloys and Compounds 356–357 (2003) 622–625.
[3] J.F.R. Castro, A.R. Yavari, A. Lemoulec, T.T. Ishikawa, W.J. BOTTA, Journal of Alloys and Compounds 389 (2005) 270–274.
[4] A.R. Yavari, A. Lemoulec, J.F.R. Castro, S. Deledda, O. Friedrichs, W.J. Botta, G. Vaughan, T. Klassen, A. Fernandez, A. Kvick, Scripta Materialia 52 (2005) 719–724.
[5] G.F. Lima, A.M. Jorge Jr., D.R. Leiva, C.S. Kiminami, C. Bolfarini, W.J. Botta, Journal of Physics: Conference Series 144 (2009) 012015, doi:10.1088/1742-6596/144/1/012015.
[6] M. Herrich, N. Ismail, J. Lyubina, A. Handstein, A. Pratt, O. Gutfleisch, Materials Science and Engineering B 108 (2004) 28–32.
[7] Songlin Li, R.A. Varin, O. Morozova, T. Khomenko, Journal of Alloys and Compounds 384 (2004) 231–248.
[8] Y. Kusadome, K. Ikeda, Y. Nakamori, S. Orimo, Z. Horita, Scripta Materialia 57 (2007) 751–753.
[9] T.T. Ueda, M. Tsukahara, Y. Kamiya, S. Kikuchi, Journal of Alloys and Compounds 386 (2005) 253–257.
[10] L. Lu, M.O. Lai, Mechanical Alloying, Klumer Academic Publishers, EUA, 1998, p. 296.